

EXPLORING ONCE-PER-REVOLUTION AUDIO SIGNAL VARIANCE AS A CHATTER INDICATOR

Tony L. Schmitz Mechanical Engineer , Kate Medicus Mechanical Engineer & Brian Dutterer Instrument Maker

To cite this article: Tony L. Schmitz Mechanical Engineer , Kate Medicus Mechanical Engineer & Brian Dutterer Instrument Maker (2002) EXPLORING ONCE-PER-REVOLUTION AUDIO SIGNAL VARIANCE AS A CHATTER INDICATOR, Machining Science and Technology, 6:2, 215-233, DOI: [10.1081/MST-120005957](https://doi.org/10.1081/MST-120005957)

To link to this article: <https://doi.org/10.1081/MST-120005957>



Published online: 16 Aug 2006.



Submit your article to this journal [↗](#)



Article views: 170



View related articles [↗](#)



Citing articles: 22 View citing articles [↗](#)



MACHINING SCIENCE AND TECHNOLOGY
Vol. 6, No. 2, pp. 215–233, 2002

EXPLORING ONCE-PER-REVOLUTION AUDIO SIGNAL VARIANCE AS A CHATTER INDICATOR

Tony L. Schmitz,* Kate Medicus, and Brian Dutterer

National Institute of Standards and Technology,
Gaithersburg, MD 20899, USA

ABSTRACT

The purpose of this study is an evaluation of the statistical variance in the once-per-revolution sampled audio signal during milling as a chatter indicator. It is shown that, due to the synchronous and asynchronous nature of stable and unstable cuts, respectively, once-per-revolution sampling leads to a tight distribution of values for stable cuts, with a corresponding low variance, and a wider sample distribution for unstable cuts, with an associated high variance. A comparison of stability maps developed using: 1) analytic techniques, and 2) the variance from once-per-revolution sampled time-domain simulations is provided and good agreement is shown. Experimental agreement between the well-known Fast Fourier Transform (FFT) chatter detection method, that analyzes the content of the FFT spectrum for chatter frequencies, and the new variance-based technique is also demonstrated.

Key Words: Milling; Stability; Chatter; Variance

INTRODUCTION

One primary limiting factor in achieving high material removal rates (MRR) in milling operations is unstable cutting, or chatter, characterized by increased forces and

*Corresponding author.

varying levels of workpiece and/or tool damage. Chatter avoidance techniques are therefore an important area of machining research. Previous studies may generally be grouped into one of three categories: 1) mechanical changes to the machine tool structure and/or tool, e.g., tuned dynamic absorbers;^[1-5] tools, holders, and spindles with increased dynamic stiffness;^[6-8] draw bar force variation;^[9] variable pitch cutters;^[10-14] and tool overhang length adjustment to tune the tool point frequency response;^[15-20] 2) intelligent selection of machining parameters, e.g., reduced regenerative chatter by appropriate spindle speed selection using stability lobe diagrams;^[21,22] and 3) active control algorithms.^[23-25]

An equally important consideration, especially for situations of unmanned machining,^[26] is the detection of chatter during milling (i.e., in-process detection). Issues that affect chatter recognition sensor selection include number of sensors required, signal to noise ratio, sensor placement, bandwidth, and sensitivity. Typical sensors include force and torque dynamometers, accelerometers, laser vibrometers, capacitive/optical displacement transducers, and microphones. However, acoustic emission (AE) sensors^[27] and continuous monitoring of spindle current, voltage, and speed to calculate the instantaneous torque and power^[26] have also been investigated. Among these, it has been suggested that the use of a microphone to capture the audio cutting signal provides the most favorable compromise between the necessary requirements.^[28] In this paper, we describe the use of synchronous sampling of the milling audio signal for chatter detection, although the described method could be applied to other sensor inputs as well. It is shown that the statistical variance in the once-per-revolution sampled cutting signal provides a quality chatter indicator. Specifically, we demonstrate that stable cuts exhibit a tight distribution in the once-per-revolution sampled audio signal (low variance), while unstable cuts present a much wider distribution (high variance).

CONCEPT DESCRIPTION

The in-process chatter detection method described here is derived from Poincaré sectioning techniques traditionally applied to problems in nonlinear dynamics. Davies et al.^[16] described the application of Poincaré sectioning to motions of the cutter during milling, where the X and Y coordinate direction displacements of the tool point during cutting (obtained using an orthogonal pair of capacitance probes located near the tool tip) were analyzed for quasi-periodic behavior. It was shown that stable, or periodic, cuts generated a series of closely grouped points in the X–Y cutting plane when the tool point motions were sampled at the spindle rotation frequency. This tight grouping of experimental values represents the Poincaré map fixed point for a periodic solution (i.e., periodic motions in continuous time history are seen as fixed points in the Poincaré map). Cuts experiencing regenerative chatter, on the other hand, tended toward an elliptical point distribution, which is indicative of quasi-periodic motion where two incommensurate frequencies are present, the chatter frequency and the tooth passing frequency in this case. Although this does not represent a strict implementation of Poincaré sectioning techniques (e.g., Poincaré sections are normally constructed using the full phase space, or all possible states, of the dynamic system), it is sufficient for classifying the nature of the tool motions. More information on

ONCE-PER-REVOLUTION AUDIO SIGNAL VARIANCE

217

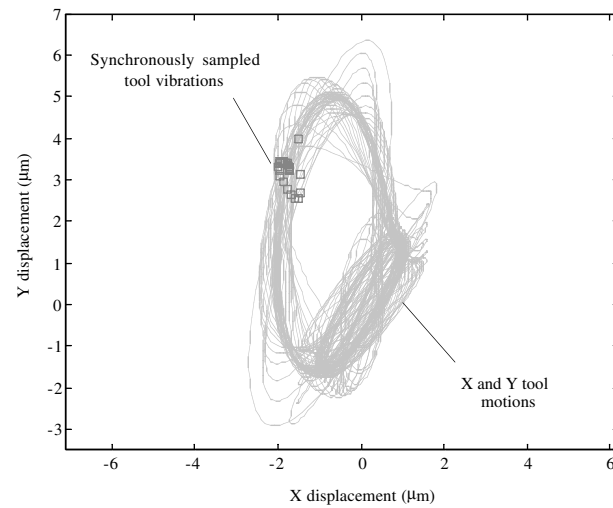


Figure 1. Example of synchronously sampled cutter motions for stable half immersion down milling cut.

Poincaré sectioning theory may be found in texts by Guckenheimer and Holmes^[29] and Moon,^[38] for instance.

Examples of the tight distribution of once-per-revolution sampled cutter motions during stable milling and elliptical distribution for unstable cutting are shown in Figures 1 and 2, respectively. These plots were generated using a modification of the time-based milling simulation described by Tlustý.^[36] Features of the simulation

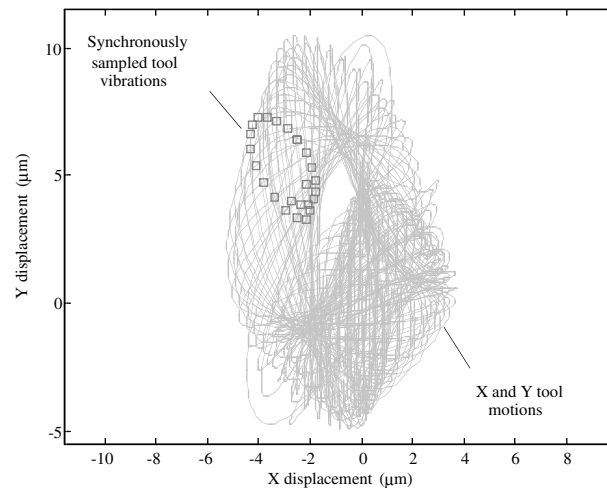


Figure 2. Example of synchronously sampled cutter motions for unstable half immersion down milling cut.

include Euler integration for tool position, calculation of the instantaneous chip thickness using multiple previous passes of the cutter (surface regeneration), and treatment of the non-linearity caused by a tooth leaving the cut during large cutter deflections. The primary assumptions include straight cutter teeth and a circular tool path. From Figures 1 and 2, it is seen that, although the tool clearly vibrates in both cases, the cutter motions are synchronous with spindle rotation (and approach the map fixed point after some initial transients) in the stable case and asynchronous for the chattering cut.

The work of Davies et al. has been extended here to include once-per-revolution sampling of the milling audio signal and a statistical evaluation of the results. The notion of a statistical interrogation of the synchronously sampled audio signal is based on the premise that stable cuts generate content synchronous with spindle rotation and, therefore, the periodically sampled audio signal will be characterized by a tightly spaced cluster of values with a low statistical variance, as shown in Figure 1. An unstable cut (due to regenerative chatter), on the other hand, demonstrates asynchronous motion and gives a more distributed set of audio samples with a corresponding larger variance, as demonstrated in Figure 2.

This analysis differs from existing audio signal examination algorithms. For example, the Chatter Recognition and Control (CRAC) system^[30] calculates the Fast Fourier Transform (FFT) of the time-based audio signal, comb filters the resulting spectrum to remove the tooth passing frequency and higher harmonics, and adjusts the spindle speed to match the dominant chatter frequency if the cut is unstable. Although the method described here does not offer the diagnostic capability of identifying alternate stable spindle speeds without additional signal processing, it does sense chatter using a much less computationally intensive procedure, i.e., the variance of the time-based signal versus the frequency-domain FFT and subsequent filtering, and operates on a much smaller data set. Specifically, only one sample per spindle revolution is required versus the tens of kilohertz sampling rates necessary to avoid aliasing in the FFT analysis. Additionally, it is not necessary to analyze the entire frequency spectrum within the selected bandwidth to search for and identify any offending chatter

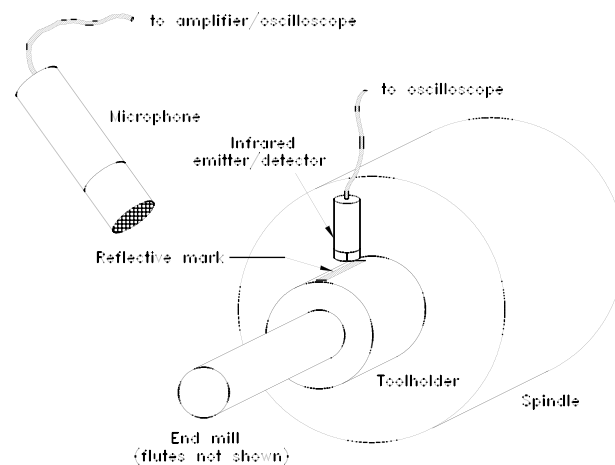


Figure 3. Experimental setup for variance-based chatter detection.

ONCE-PER-REVOLUTION AUDIO SIGNAL VARIANCE

219

frequencies; it is only required that a single scalar quantity, the variance in the synchronously sampled cutting data, be considered. These benefits make it a prime candidate for real-time, remote condition-based monitoring of milling processes.

The setup used in this research for implementation of the variance-based chatter detection method is shown in Figure 3. The required hardware, which was mounted on a high-speed, horizontal spindle (20,000 rpm/20 kW) machining center located in the NIST instrument fabrication shop, included a unidirectional microphone (Optimus 33-3023) mounted inside the machine enclosure, microphone amplifier (PCB 482A17),¹ once-per-revolution signal generator comprised of an infrared emitter/detector pair and reflective tool mark, and a digital oscilloscope for collection of the time-based audio and once-per-revolution signals. Post-processing of the data included sampling the audio signal using the once-per-revolution 'trigger' and calculating the variance, s^2 , in N synchronously sampled values, r_i , according to Eq. 1, where r_m is the mean or arithmetic average of the samples. Strictly speaking, the use of Eq. 1, which provides the moment of inertia of the observations r_i , implies the existence of reasonably symmetric bell-shaped histograms,^[31] but the assumption here is that it is used only as a metric to track changes in the spread of the synchronously sampled audio data.

$$s^2 = \frac{\sum_{i=1}^N (r_i - r_m)^2}{N - 1}, \quad \text{where } r_m = \frac{\sum_{i=1}^N r_i}{N} \quad (1)$$

A preferred setup for industrial applications would include use of the microphone and access to the spindle encoder's once-per-revolution signal to sample the audio data, employing available data acquisition channels in the machine tool controller or a data acquisition card in a local personal computer. This sampled data could then be represented in either: 1) a real-time display, similar to the frequency-based LED output seen in various stereo equalizers, that shows a continuously-updated histogram indicating the process stability (i.e., a tight distribution for stable cutting or broader distribution for unstable conditions as illustrated in Figure 4); or 2) a trend line showing the calculated variance during a machining operation.^[32] The identification of chatter using data represented in either of these manners would require no knowledge of the machine dynamics, process specific cutting energy coefficients, process parameters, or vibrations theory and could potentially reduce the difficulties associated with the practical implementation of high-speed machining on the shop floor.

The selection of a microphone as the chatter sensor in this work is based on several considerations, as detailed by Delio et al.^[28] First, it is possible to place the sensor in reasonable proximity to the process. This limits the filtering effects of components between the process and sensor (e.g., coloring of the cutting signal by the

¹Commercial equipment is identified in order to adequately specify certain procedures. In no case does such identification imply recommendation or endorsement by the National Institute of Standards and Technology, nor does it imply that the equipment identified is necessarily the best available for the purpose.

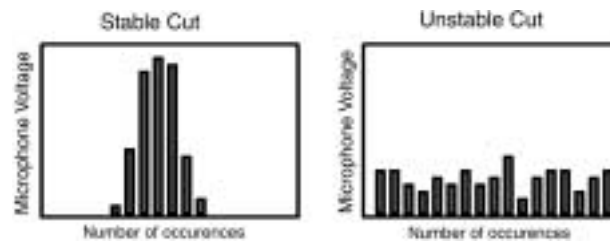


Figure 4. Example outputs for real-time LED display of synchronously sampled cutting data.

machine tool structure before it reaches a remotely placed accelerometer). Second, only one sensor is required to fully diagnose the process health. Third, improved sensitivity to chatter in situations of low force or radial immersion compared to force-based sensors has been demonstrated.^[28] Fourth, the issue of placing a motion-based sensor on a structural nodal point of the chattering mode, and the corresponding loss in sensitivity to instability, is avoided.

It should also be noted, however, that there are also limitations associated with audio detection of the cutting signal. Two important considerations are: 1) microphone bandwidth, and 2) environmental noise. In general, microphones do not offer a linear response at frequencies below approximately 100 Hz.^[28] Therefore, it may not be possible to detect chatter at very low frequencies, such as those corresponding to structural modes of large machine tools. Also, excessive noise in the machine environment could corrupt the audio signal.^[28,37] In this situation, various isolation methods may be employed to improve the signal to noise ratio. These techniques include both absorption and collection.^[28] In the absorption method, the microphone is located within a properly sized enclosure covered with absorptive material. The enclosure rejects signals, within some frequency bandwidth, that emanate from directions other than the desired signal. The collection method uses a reflector, typically parabolic in shape, to focus normally incident sound waves (from the cutting process) onto the microphone. In this research, no isolation methods were employed.

CONCEPT EVALUATION

The feasibility of using the variance in the synchronously sampled audio signal as a chatter indicator was evaluated in two parts. First, a long slender end mill, previously employed in a deep pocket high-speed milling application, was selected, its frequency response measured in the vertical and horizontal directions using impact testing (i.e., an accelerometer, instrumented hammer, and signal analyzer were used to record the ratio of the complex displacement to input force), and analytic stability lobes computed. Using the measured tool dynamics and selected cutting parameters, time-domain simulations were also completed to determine the variance in the once-per-revolution sampled resultant tool displacement at a grid of points encompassing the same range of spindle speeds and axial depths as the analytic stability lobes. This stability map was then compared to the analytic lobes. Selected cuts were also performed to locate the experimental stability boundary at the top spindle speed and verify the predicted



ONCE-PER-REVOLUTION AUDIO SIGNAL VARIANCE

221

results. In addition, an analysis was completed to explore the time-dependence of the variance as the machining conditions change during a particular cut. This work is described in Evaluation Part I.

Second, a short overhang production end mill was selected. A grid of points, covering spindle speeds and axial depths typical for this tool, was then chosen and half-immersion cuts completed at each point, while recording the once-per-revolution and audio signals. Analyses of both the audio signal FFT and variance of the synchronously sampled audio record for each cut were completed and the results compared. Additionally, sequences of cuts with small increments in spindle speed (while holding axial depth constant) and axial depth (with constant spindle speed) were completed near stability boundaries. These results are outlined in Evaluation Part II.

Evaluation Part I

The first step in evaluating the validity of using the variance in synchronously sampled machining data as a chatter indicator was to compare the stability maps obtained using existing analytic methods^[33–35] and the variance based technique. Sample slotting cuts in 7075-T6 aluminum (with specific cutting energy coefficients of 600 MPa and 0.3) were then performed to verify the boundaries predicted by both stability prediction methods. The selected cutting tool was a 12.7 mm diameter (11.8 mm relieved shank diameter) two flute, helical carbide end mill with a 104 mm overhang from the collet holder face (HSK 63A holder/spindle interface). The natural frequency, modal stiffness, and damping ratio for this cutter are given in Table 1. The measured response was symmetric in the X and Y directions, which defined the cutting plane for the machining tests.

For the development of the stability maps, a spindle speed/axial cutting depth parameter space was first selected: spindle speeds between 5000 and 21,000 rpm and axial depths of cut from zero to 1.0 mm. Analytic stability lobes were then calculated^[33] and time-domain simulations executed over a grid of points in the selected parameter space (100 rpm spindle speed resolution and 1 μ m axial depth resolution). The variance for each of the spindle speed/axial depth pairs tested was calculated by: 1) recording the discretized resultant cutter deflection, $r(kT)$ where k is an integer and T is the simulation sampling interval, over many cutter revolutions; 2) once-per-revolution sampling the set of $r(kT)$ values; and 3) applying Eq. 1 to the part 2) result. The calculation of the resultant cutter deflection is shown in Eq. 2, where $x(kT)$

Table 1. 12.7 mm Diameter, 104 mm Overhang End Mill Modal Parameters

Modal Parameter	Value
Natural frequency, f_n	922 Hz
Stiffness, k	1.34×10^6 N/m
Viscous damping ratio, ζ	0.011

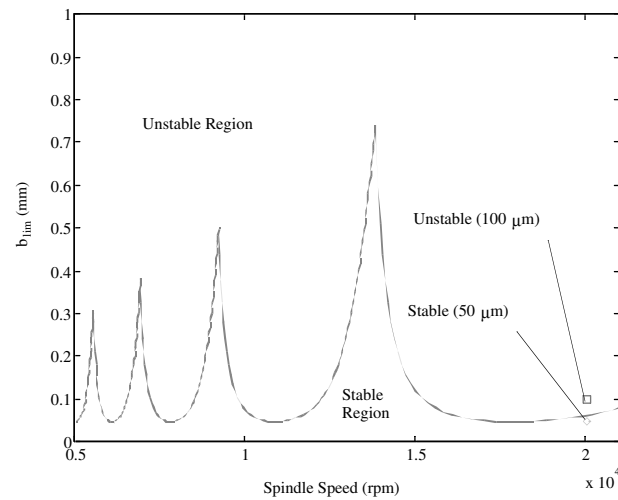


Figure 5. Analytic stability lobes for slotting with 12.7 mm diameter, 104 mm overhang end mill.

and $y(kT)$ are the discretized time-based cutter deflection in the X and Y directions, respectively and K is the total number of simulation steps.

$$r(kT) = \sqrt{x(kT)^2 + y(kT)^2}, \quad k = 1 \text{ to } K \quad (2)$$

The analytic stability lobes and variance-based stability map are shown in Figures 5 and 6, respectively. The analytic stability lobes separate unstable cutting

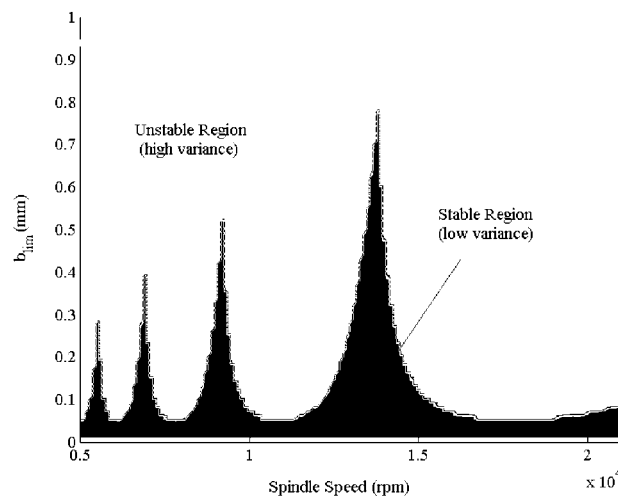


Figure 6. Variance-based stability map for slotting with 12.7 mm diameter, 104 mm overhang end mill.



ONCE-PER-REVOLUTION AUDIO SIGNAL VARIANCE

223

regions (above the curve) from unstable zones (below the curve). The variance-based stability map is a contour plot viewed in the spindle speed/axial depth of cut plane. Stable zones are represented by low variance values (black) and unstable zones are denoted by high variance values (white). Good agreement between the two methods is demonstrated. A qualitative comparison is given in Table 2, where the most favorable spindle speeds and corresponding allowable axial depths are recorded. It should be noted that the spindle speed resolution selected for the time-domain simulation grid (100 rpm) limits the agreement between the two methods.

To partially verify the approximate scaling of the analytic and variance-based stability maps, slotting cuts were performed at axial depths slightly above (100 μm) and below (50 μm) the stability limit at the top available spindle speed (20,000 rpm). These cuts are identified in Figure 5. The audio and once-per-revolution signals were captured using the setup shown in Figure 3. The audio signal was anti-alias low pass filtered at 5 kHz prior to being sampled at 20 kHz. The once-per-revolution signal was also sampled at 20 kHz. During the cutting tests, chatter was evident for the 100 μm cut, while the 50 μm was stable. Histograms of the synchronously sampled audio data for the stable and unstable cuts are shown in Figures 7A and 8A, respectively. Clearly, the spread in the data for the chattering and stable cuts differs substantially. Quantitatively, the variance in the 100 μm data was 17.5 times higher than the 50 μm cut variance. FFT spectrums for the two cuts are shown in Figures 7B and 8B. The unstable cut in Figure 8B shows a peak at the chatter frequency (near the tool's natural frequency), while the stable exhibits content only at the tooth passing frequency and its harmonics (see Figure 8A).

A common situation encountered in pocketing operations is a short duration of chatter, or a characteristic 'squeak', in the corners as the radial immersion increases. A schematic of the increase from 50% to 100% radial immersion (RI) as the tool enters a pocket corner is shown in Figure 9. The time-dependence of the variance in the synchronously sampled data during this increase in RI was explored using time-domain simulation. The same cutter modal parameters and specific cutting energy coefficients used to develop the analytic and variance-based stability maps shown in Figures 5 and 6 were again applied. The selected cutting conditions were: 1.5 mm axial depth, 13,800 rpm spindle speed (near the center of the highest available lobe for the selected cutter dynamics), and 0.1 mm feed/tooth. This axial depth is stable for the 50% RI cut, but unstable in the slotting case.

The milling simulation proceeded by entering the 50% RI cut at time, t , equal to zero. The cut proceeded for 10 mm (50 cutter revolutions or 0.217 s) at 50% RI. The

Table 2. Quantitative Comparison Between Analytic and Variance-Based Stability

Analytic Stability Lobes		Variance-Based Stability Map	
Spindle Speed (rpm)	Axial Depth (mm)	Spindle Speed (rpm)	Axial Depth (mm)
13834	0.74	13,800	0.78
9224	0.50	9200	0.52
6919	0.38	6900	0.39
5536	0.31	5500	0.28

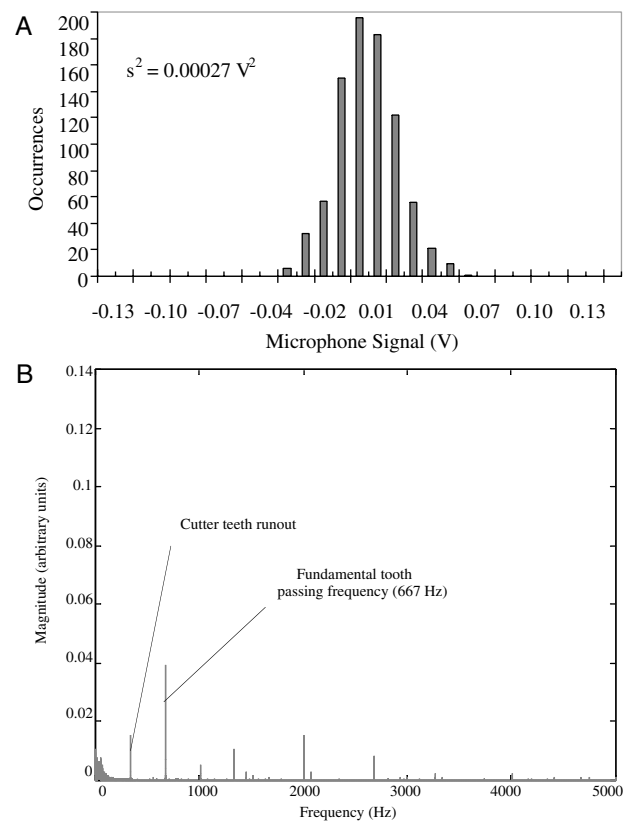


Figure 7. (A) Histogram for stable 50 μm axial depth slotting cut using 12.7 mm diameter, 104 mm overhang end mill. (B) FFT spectrum for stable 50 μm axial depth slotting cut using 12.7 mm diameter, 104 mm overhang end mill.

radial immersion then began increasing by decreasing the entry angle, ϕ_{entry} (defined in Figure 9), of the teeth into the cut from 90° to 0° according to Eq. 3. In this equation, R is the cutter radius (6.35 mm) and f_r is the linear feed rate (46 mm/s). The exit angle of the teeth leaving the cut was maintained at a constant value of 180° .

$$\phi_{entry} = \sin^{-1}\left(\frac{R - f_r(t - 0.217)}{R}\right) \quad (3)$$

The simulation results are shown in Figures 10 and 11. Figure 10 shows the time-domain X and Y direction tool vibrations as the cut was carried out. After some initial transients, steady-state vibration amplitudes are reached in each direction. A second transitory period is reached when the RI begins increasing at a time of 0.217 s. Fully developed chatter eventually occurs. Figure 11 shows the corresponding changes in the variance of the once-per-revolution sampled resultant vibration (a 230 Hz sampling frequency is required for this spindle speed). This variance was calculated according to

ONCE-PER-REVOLUTION AUDIO SIGNAL VARIANCE

225

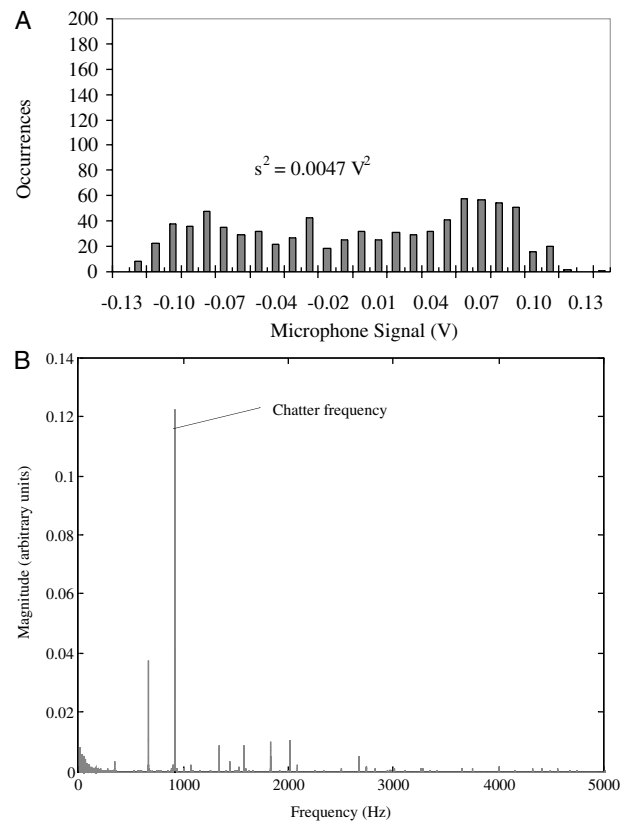


Figure 8. (A) Histogram for unstable 100 μm axial depth slotting cut using 12.7 mm diameter, 104 mm overhang end mill. (B) FFT spectrum for unstable 100 μm axial depth slotting cut using 12.7 mm diameter, 104 mm overhang end mill.

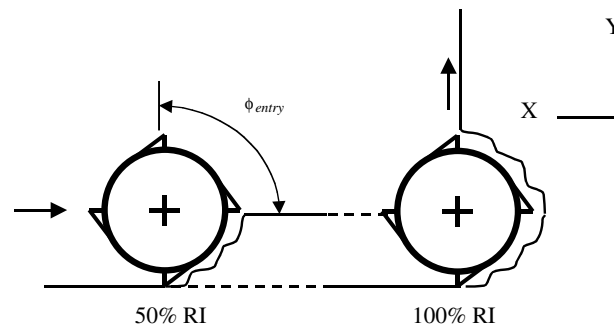


Figure 9. Increase in radial immersion as tool enters corner of pocketing contour.

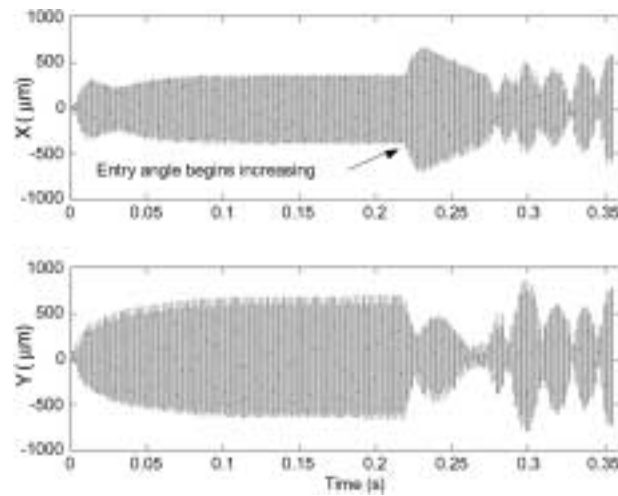


Figure 10. Time-domain cutter vibrations in X and Y directions.

Eq. 1 using a moving window of 20 samples (for this spindle speed an update rate of 11.5 Hz would be required). It can be seen in the figure that there is a rapid decrease in the variance as steady-state conditions are reached. The final value before the RI begins increasing is $0.15 \mu\text{m}^2$. As the entry angle begins decreasing, a sharp rise in the variance then occurs due to the transient behavior. The variance continues to increase to a maximum value of $31,272 \mu\text{m}^2$ as chatter develops and the 100% RI is reached

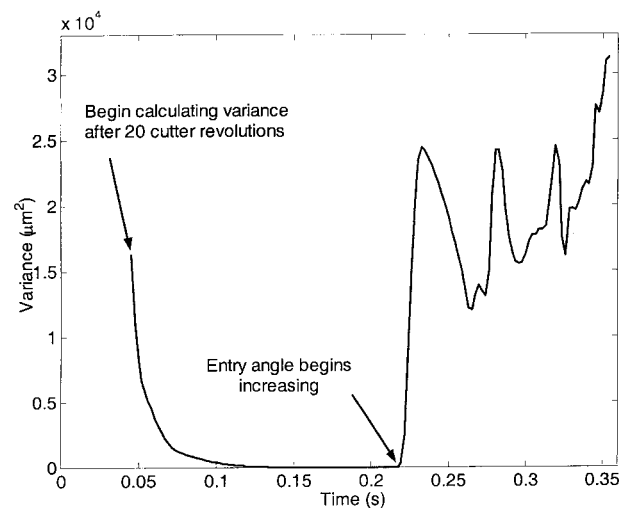


Figure 11. Time-dependent variance for cut with increasing radial immersion (20 sample variance calculation window).

ONCE-PER-REVOLUTION AUDIO SIGNAL VARIANCE

227

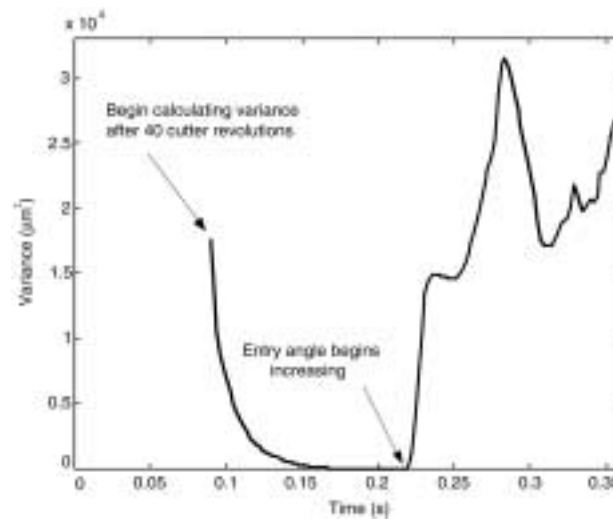


Figure 12. Time-dependent variance for cut with increasing radial immersion (40 sample variance calculation window).

($t=0.355$ s). Two conclusions can be drawn from these results. First, transient behavior during cutting could lead to false chatter identification if high update rates are used. A longer variance calculation window could reduce the sensitivity to transients, but may also increase the time chatter is allowed to continue before detection. As an example, the variance calculated using a 40 sample moving window is shown in Figure 12. It is seen that the initial transients still affect the starting variance value, but it drops off more rapidly than the 20 sample case. Also, the oscillations in the calculated variance after the second transitory period are reduced with the longer window. Second, the variance-based method is agile enough to detect the common problem of chattering in corners during pocketing operations.

Evaluation Part II

In the second portion of the variance-based chatter detection evaluation, a 12.7 mm diameter, two flute, helical carbide end mill with a 44 mm overhang was selected to perform a number of half immersion down milling cutting tests covering spindle speeds (14,000 rpm to 18,000 rpm) and axial depths (2.03 mm to 5.08 mm) typical for this tool. In all cases, a constant feed per tooth of $102 \mu\text{m}$ was maintained. The purpose of these tests was to verify agreement between the well-established FFT-based chatter sensing algorithm and the variance-based method over a large range of stable and unstable cuts. The microphone and once-per-revolution sampling data were again obtained using the setup shown in Figure 3. In this case, the microphone signal was low pass filtered at 7 kHz and both the microphone and once-per-revolution signals sampled at 50 kHz.

Axial Depth (mm)	5.08	12	2474	27	29	29
	4.32	22	1398	53	57	25
	3.56	12	709	28	70	34
	2.79	17	48	41	31	22
	2.03	37	26	72	25	35
		14000	15000	16000	17000	18000
		Spindle Speed (rpm)				

Figure 13. Once-per-revolution variance stability results for half immersion cuts using 12.7 mm diameter, 44 mm overhang end mill (unstable cuts identified by bold lines).

Results for the once-per-revolution variance and FFT analyses are shown in Figures 13 and 14, respectively, where unstable cuts have been identified with bold lines around the appropriate grid locations. Figure 13 displays the value of the calculated variance (in mV^2) for each of the twenty-five spindle speed/axial depth pairs. The cutoff point between stable and unstable cuts, i.e., the analysis calibration, can be selected by multiplying the variance for an arbitrary stable cut by some pre-selected value. Our experience suggests that 7 is a reasonable choice since the recorded variance for unstable cuts is typically at least an order of magnitude larger than the variance for stable cuts. The magnitude of the fundamental chatter frequency from the FFT analysis (in arbitrary units), provided one existed after comb filtering, is shown in Figure 14. If a chatter frequency was not evident above the noise floor (selected at a level of 0.002), the value was set to zero. This noise floor selection effectively serves as the calibration for the FFT data and must be performed each time there are changes in the process parameters. In both cases, chatter is clearly recognized for 15,000 rpm cuts at axial depths equal to and exceeding 3.56 mm. At a 2.79 mm axial depth for the same spindle speed, the chatter peak is just visible above the FFT noise floor, but the variance value does not suggest instability.² Aside from this data point, the once-per-revolution variance and FFT spectrum results demonstrate good agreement.

It is also noteworthy that the variance values continue to grow as the axial depth is increased, while the fundamental chatter frequency magnitude does not grow between the 4.32 mm and 5.08 mm axial depth cuts. This can be attributed to the nature of the FFT spectrum for the unstable cuts. In each case, the spectrum shows frequency

²Note that the noise floor in this case was post-process selected with a priori knowledge of the stability behavior in order to provide the most rigorous evaluation of the variance-based method. The selection of a slightly higher noise floor would not have detected chatter at this depth.

ONCE-PER-REVOLUTION AUDIO SIGNAL VARIANCE

229

Axial Depth (mm)	5.08	0	0.025	0	0	0
4.32	0	0.026	0	0	0	
3.56	0	0.015	0	0	0	
2.79	0	0.005	0	0	0	
2.03	0	0	0	0	0	
		14000	15000	16000	17000	18000
		Spindle Speed (rpm)				

Figure 14. FFT stability analysis results for half immersion cuts using 12.7 mm diameter, 44 mm overhang end mill (unstable cuts identified by bold lines).

modulation of the chatter signal at the tooth passing frequency (i.e., sidebands of the fundamental chatter frequency near 3840 Hz are seen spaced at the tooth passing frequency). This is the result of both forced and self-excited vibrations occurring simultaneously and is demonstrated by the FFT spectrum for the 5.08 mm axial depth, 15,000 rpm cut shown in Figure 15.

As noted previously, additional half immersion down milling cuts were performed in smaller increments of spindle speed and axial depth near the stability boundaries located from the group of cutting tests detailed in Figures 13 and 14.

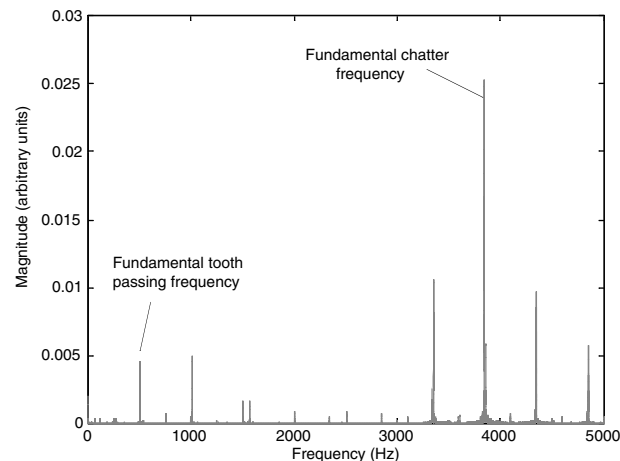


Figure 15. FFT spectrum for unstable 15,000 rpm, 5.08 mm axial depth half immersion cut using 12.7 mm diameter, 44 mm overhang end mill.

Table 3. Constant Axial Depth/Varying Spindle Speed Cutting Tests for 12.7 mm Diameter, 44 mm Overhang Cutter (Unstable Cuts Are Identified by Bold Font)

Spindle Speed (rpm)	Once-Per-Revolution Variance (mV^2)	Fundamental Chatter Frequency Amplitude (Arbitrary Units)
14,000	35	0
14,100	15	0
14,200	14	0
14,300	24	0
14,400	18	0
14,500	36	0
14,600	20	0
14,700	904	0.028
14,800	1758	0.030
14,900	2277	0.017
15,000	2040	0.034

Table 3 shows the results for constant axial depth (5.08 mm)/varying spindle speed (100 rpm increments from 14,000 rpm to 15,000 rpm) tests. For both the variance-based and FFT analyses, the stability boundary at the selected axial depth was determined to be 14,700 rpm.

Sample results for the constant spindle speed (15,000 rpm)/varying axial depth tests are shown in Figures 16 and 17. These figures display height maps, or topographs, of the machined surface left by the tool's periphery. They were obtained using a scanning white light interferometer with a 2.5x objective magnification and 2.8 mm by 3.7 mm field of view. Figure 16 shows the result for a stable 2.69 mm axial depth cut. The average roughness, or R_a , value calculated from this map was $1.07 \mu\text{m}$. The variance in the once-per-revolution sampled audio signal for this axial depth was 9 mV^2 ; no chatter frequency was detected in the FFT spectrum. The height map for an unstable cut (axial depth of 2.90 mm) is shown in Figure 17. The average roughness

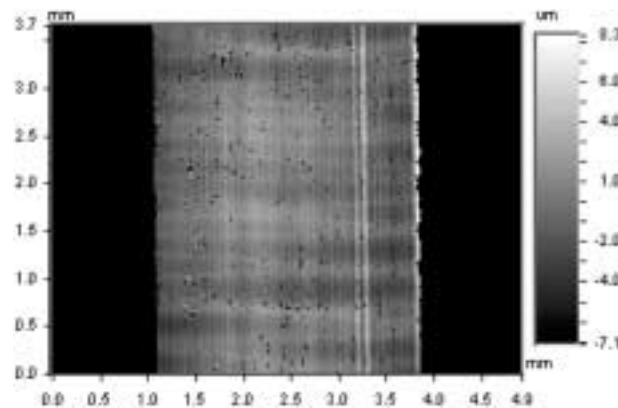


Figure 16. Surface finish for stable 15,000 rpm, 2.69 mm axial depth half immersion cut using 12.7 mm diameter, 44 mm overhang end mill.

ONCE-PER-REVOLUTION AUDIO SIGNAL VARIANCE

231

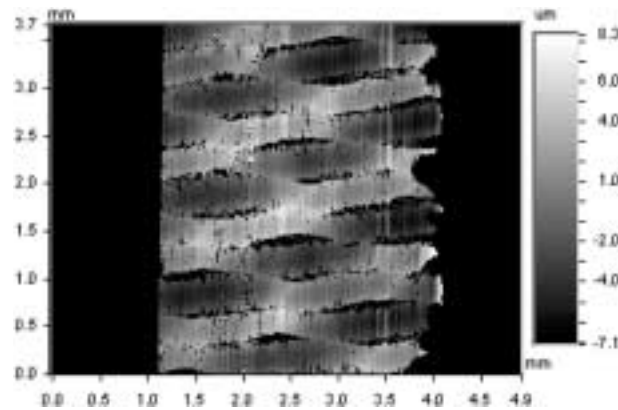


Figure 17. Surface finish for unstable 15,000 rpm, 2.90 mm axial depth half immersion cut using 12.7 mm diameter, 44 mm overhang end mill.

has now increased to $2.27 \mu\text{m}$ and the chatter marks are evident. In this case, a variance of 160 mV^2 was calculated, a nearly 18 times increase over the previous stable cut, and the amplitude of the fundamental chatter frequency was 0.010 (arbitrary units). Collectively, these two cuts bound the axial depth stability limit shown in Figure 14.

CONCLUSIONS

A new chatter detection technique, based on the statistical variance in the once-per-revolution sampled audio signal during milling, is described. This method uses the synchronous and asynchronous nature of stable and unstable cuts, respectively, to identify chatter. Specifically, it relies on the fact that stable cuts generate content synchronous with spindle rotation and, therefore, the periodically sampled milling signal is characterized by a tightly spaced cluster of values with a corresponding low statistical variance. Unstable cuts caused by regenerative chatter, however, demonstrate asynchronous motion and give a more distributed set of samples with a subsequently larger variance when once-per-revolution sampled. A comparison of stability maps developed using: 1) analytic techniques, and 2) the variance from once-per-revolution sampled time-domain simulations, is provided and good agreement is shown. Experimental agreement between the well-known Fast Fourier Transform chatter detection method and the new variance-based technique is also demonstrated.

ACKNOWLEDGMENTS

The authors would like to acknowledge technical contributions and helpful suggestions from Drs. Matthew Davies (NIST, Gaithersburg, MD), Jon Pratt (NIST, Gaithersburg, MD), Phil Bayly (Washington University in St. Louis, St. Louis, MO), and Scott Smith (University of North Carolina at Charlotte, Charlotte, NC) and Mr. Jerry Halley (The Boeing Company, St. Louis, MO).



REFERENCES

1. den Hartog, J. *Mechanical Vibrations*; Dover Publications, Inc.: New York, New York, 1985.
2. Klein, R.; Nachtigal, C. A theoretical basis for the active control of a boring bar operation. *Trans. ASME: J. Dyn. Syst., Meas., Control* **1975**, *97*, 172–178.
3. Glase, D.; Nachtigal, C. Development of a hydraulic chambered, actively controlled boring bar. *Trans. ASME, Ser. B* **1979**, *101*, 362–368.
4. Tewani, S.; Rouch, K.; Walcott, B. A study of cutting process stability of a boring bar with active dynamic absorber. *Int. J. Mach. Tools Manuf.* **1994**, *35/1*, 91–108.
5. Chung, B.; Smith, S.; Tlusty, J. Active damping of structural modes in high-speed machine tools. *J. Vib. Controls* **1997**, *3*, 270–295.
6. Weck, M.; Schubert, I. New interface machine/tool: Hollow shank. *Ann. CIRP* **1994**, *43/1*, 345–348.
7. Agapiou, J.; Riving, E.; Xie, C. Toolholder/spindle interfaces for CNC machine tools. *Ann. CIRP* **1995**, *44/1*, 383–387.
8. Weck, M.; Hennes, N.; Krell, M. Spindle and toolsystems with high damping. *Ann. CIRP* **1999**, *48/1*, 297–302.
9. Smith, S.; Jacobs, T.; Halley, J. The effect of drawbar force on metal removal rate in milling. *Ann. CIRP* **1999**, *48/1*, 293–296.
10. Slavicek, J. *The Effect of Irregular Tooth Pitch on Stability of Milling*; Proceedings of the 6th MTDR Conference. Pergamon Press: London, 1965; 15–22.
11. Tlusty, J.; Ismail, F.; Zaton, W. Use of special milling cutters against chatter. *Trans. NAMRI/SME* **1983**, *11*, 408–415.
12. Vanherck, P. *Increasing Milling Machine Productivity by Use of Cutters with Non Constant Cutting Edge Pitch*; Proceedings of the 8th MTDR Conference. Pergamon Press: Manchester, 1967; 947–960.
13. Altintas, Y.; Engin, S.; Budak, E. Analytical stability prediction and design of variable pitch cutters. *Trans. ASME J. Manuf. Sci. Eng.* **1999**, *121*, 173–178.
14. Budak, E. Improving productivity and part quality in milling of titanium based impellers by chatter suppression and force control. *Ann. CIRP* **2000**, *49/1*, 31–36.
15. Tlusty, J.; Smith, S.; Winfough, W. Techniques for the use of long slender end mills in high-speed machining. *Ann. CIRP* **1996**, *45/1*, 393–396.
16. Davies, M.; Dutterer, B.; Pratt, J.; Schaut, A. On the dynamics of high-speed milling with long, slender endmills. *Ann. CIRP* **1998**, *47/1*, 55–60.
17. Smith, S.; Winfough, W.; Halley, J. The effect of tool length on stable metal removal rate in high speed milling. *Ann. CIRP* **1998**, *47/1*, 307–310.
18. Schmitz, T.; Donaldson, R. Predicting high-speed machining dynamics by sub-structure analysis. *Ann. CIRP* **2000**, *49/1*, 303–308.
19. Schmitz, T.; Davies, M.; Medicus, K.; Snyder, J. Improving high-speed machining material removal rates by rapid dynamic analysis. *Ann. CIRP* **1999**, *50/1*, 263–268.
20. Schmitz, T.; Davies, M. Tool point frequency response prediction for high-speed machining by RCSA. *J. Manuf. Sci. Eng.* **2001**, *123*, 700–707.
21. Smith, S.; Delio, T. Sensor-Based Control for Chatter-Free Milling by Spindle Speed Selection. In *Symposium on Control Issues in Manufacturing*; 1989; DSC-Vol. 18, ASME, WAM.



ONCE-PER-REVOLUTION AUDIO SIGNAL VARIANCE

233

22. Smith, S.; Tlusty, J. Stabilizing chatter by automatic spindle speed regulation. *Ann. CIRP* **1992**, *41/1*, 433–436.
23. Takemura, T.; Kitamura, T.; Hoshi, T. Active suppression of chatter by programmed variation of spindle speed. *Ann. CIRP* **1974**, *23/1*, 121–122.
24. Weck, W.; Verhaag, E.; Gather, M. Adaptive control for face-milling operations with strategies for avoiding chatter vibrations and for automatic cut distribution. *Ann. CIRP* **1975**, *24/1*, 405–409.
25. Sexton, J.; Stone, B. The stability of machining with continuously varying spindle speed. *Ann. CIRP* **1978**, *27/1*, 321–326.
26. Tlusty, J.; Andrews, G. A critical review of sensors for unmanned machining. *Ann. CIRP* **1983**, *33/2*, 563–572.
27. Inasaki, I. Application of acoustic emission sensor for monitoring machining processes. *Ultrasonics* **1998**, *36*, 273–281.
28. Delio, T.; Tlusty, J.; Smith, S. Use of audio signals for chatter detection and control. *Trans. ASME, Ser. B* **1992**, *114*, 146–157.
29. Guckenheimer, J.; Holmes, P. *Nonlinear Oscillations, Dynamical Systems, and Bifurcations of Vector Fields*; Springer-Verlag: New York, 1983.
30. Winfough, W.; Smith, S. Automatic selection of the optimum metal removal conditions for high-speed milling. *Trans. NAMRI/SME* **1995**, *23*, 163–168.
31. Bowker, A.; Lieberman, G. *Engineering Statistics*; Prentice-Hall Inc.: Englewood Cliffs, New Jersey, 1959.
32. Schmitz, T.; Davies, M. In-Process Chatter Avoidance Display. NIST Docket No. 01-014PA, Application for U.S. Patent, submitted April, 2001.
33. Altintas, Y.; Budak, E. Analytical prediction of stability lobes in milling. *Ann. CIRP* **1995**, *44/1*, 357–362.
34. Altintas, Y.; Lee, P. A general mechanics and dynamics model for helical end mills. *Ann. CIRP* **1996**, *45/1*, 59–64.
35. Budak, E.; Altintas, Y. Analytical prediction of chatter stability conditions for multi-degree of freedom systems in milling, Part I: Modeling, Part II: Applications. *Trans. ASME: J. Dyn. Syst., Meas., Control* **1998**, *120*, 22–36.
36. Tlusty, J. *Manufacturing Processes and Equipment*; Prentice Hall: Upper Saddle River, New Jersey, 1999.
37. Weck, M.; Melder, W. Problems in assessing the noise behavior of machine tools. *Ann. CIRP* **1977**, *26/2*, 397–402.
38. Moon, F. *Chaotic Vibrations*; John Wiley & Sons: New York, 1987.